Imaging techniques for research and education of thermal and mechanical interactions of lasers with biological and model tissues

Rudolf M. Verdaasdonk
Christiaan F. P. van Swol
Matthijs C. M. Grimbergen
Alex I. Rem
University Medical Center, Utrecht
Department of Medical Physics
P.O. Box 85500
Zip 3508 GA
Utrecht, The Netherlands
E-mail: r.m.verdaasdonk@umcutrecht.nl

Abstract. A setup based on color Schlieren techniques has been developed to study the interaction of energy sources, such as lasers, with biological tissues. This imaging technique enables real-time visualization of dynamic temperature gradients with high spatial and temporal resolution within a transparent tissue model. High-speed imaging techniques were combined in the setup to capture mechanical phenomena such as explosive vapor, cavitation bubbles, and shock waves. The imaging technique is especially used for qualitative studies because it is complex to obtain quantitative data by relating the colors in the images to temperatures. By positioning thermocouples in the field of view, temperature figures can be added in the image for correlation to colored areas induced by the temperature gradients. The color Schlieren setup was successfully used for various studies to obtain a better understanding of interaction of various laser, rf, and ultrasound devices used in medicine. The results contributed to the safety and the optimal settings of various medical treatments. Although the interaction of energy sources is simulated in model tissue, the video clips have proven to be of great value for educating researchers, surgeons, nurses, and students to obtain a better understanding of the mechanism of action during patient treatment. © *2006 Society of Photo-Optical Instrumentation Engineers.* [DOI: 10.1117/1.2338817]

1 Introduction

Over the years many studies have been conducted involving the basic interaction of laser light and other energy sources with biological tissues to obtain a better understanding of the processes involved. These processes can be a combination of optical, thermal, and mechanical effects depending on the energy applied per unit of volume per unit of time.

The dominating effect is the conversion of light to thermal energy resulting in a temperature rise in the tissue.[1] In general, continuous wave lasers heat up the tissue gradually and thermal energy is conducted to the environment. Pulsed lasers, however, heat up the tissue instantly over $100\,°C$ creating an explosive vapor that results in mechanical effects. When the vapor condensates, thermal energy is released and dissipated in the tissue. To control the direct effect and predict the outcome of a clinical procedure, it is important to understand the dissipation of the thermal energy in tissue. Therefore, the characteristics of lasers and settings in tissues are being studied using various temperature measuring techniques. Most commonly, either thermocameras or thermo-

couples are being used for temperature measurements. Both have limitations as to resolution or interference with the medium of interest.[2] To study the mechanical effects of pulsed lasers, high-speed imaging techniques are used.

In this paper, a multipurpose setup is described that has been developed and applied for many years by the authors[3] for real-time visualization of thermal and mechanical effects of continuous wave lasers, pulsed lasers, and other energy sources, generating electrical currents or cavitation bubbles, during interaction with tissues with both a high temporal and a spatial resolution. The images have proven to be useful to obtain a better understanding of laser-tissue interaction and to be a great education tool for researchers, surgeons, nurses, and students.

2 Techniques for Temperature Measurements

2.1 Invasive Temperature Measurements

Thermocouples, thermistors, and silicon-based sensors are commonly used to measure temperatures invasively. The principle of the sensors is either based on the temperature dependence of contact voltage or resistance between two materials. Their characteristics are described in detail elsewhere.[4–6]

Address all correspondence to Rudolf Verdaasdonk, Clinical Physics, F01.125, University Medical Center Utrecht, P.O. Box 85500, Utrecht, 3508 GA, Netherlands; Tel: +31 30 2507302; Fax: +31 30 2542002; E-mail: r.m.verdaasdonk@umcutrecht.nl
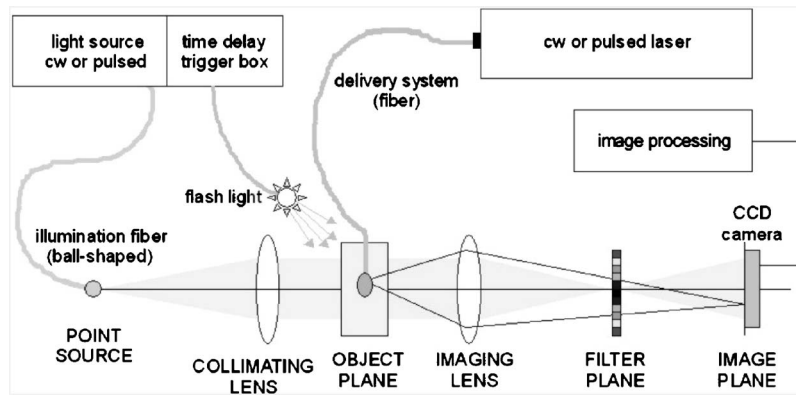
Fig. 1 Schematic of the components of a color Schlieren setup to study laser-tissue interaction.

Small sensors can be positioned invasively underneath the tissue surface to monitor the temperature at one position in time. Accuracy within $0.1\,°C$ can be achieved if precautions are taken to shield interference from the environment. Although the sensors can be as small as $100\ \mu m$, they are still interfering with the environment when used invasively. During laser irradiation, the sensor can absorb light itself, resulting in an error of the temperature reading. By irradiating the tissue intermittently, it is possible to correct for this error.[7] Invasive sensors provide a temperature reading at one position only, which is a limitation to determine temperature distributions during laser-tissue interaction.

2.2 Noninvasive Temperature Measurements

Temperature measurements without touching the object are typically performed using infrared sensors detecting the "heat" irradiated by the object. This technique, thermography, has been used in medicine for many years to measure skin temperature distribution providing information on blood perfusion for diagnosing or detecting malignancies.[8,9] Infrared cameras have been used for many years and technology has greatly improved the detectors and method of cooling. Smart software packages and libraries enable correction for material characteristics and emissivity to obtain calibrated temperatures. However, only temperatures at a surface can be visualized, which is a limitation of the ir camera when studying laser-tissue interaction.[2] However, the data at the surface is useful to extrapolate to temperature distribution underneath the surface.

There are three emerging techniques to measure temperatures inside tissue in a noninvasive way: magnetic resonance imaging (MRI), microwave radiometry, ultrasound thermometry.

MRI has proven to be a very promising technique to monitor temperature changes for diagnosis and during minimal invasive treatments.[10,11] The proton resonance frequency (PRF) used for MRI has a linear temperature dependency and is relatively independent for tissue type. These characteristics make PRF a perfect technique for temperature measurements in real time. At this moment, a resolution of $1\,°C$, within 1 s in a tissue area of 2 mm is achieved; however, with evolving techniques, higher resolutions can be expected in near future.

Another technique is based on microwave radiometry.[12] By measuring the microwave electromagnetic thermal noise, tem-

perature information can be obtained. This technique is able to provide temperature information at a depth of up to several centimeters in subcutaneous tissues.

The use of ultrasound for noninvasive thermometry is under investigation.[13–15] In theory it should be possible to acquire temperature data by measuring thermally induced modifications in backscattered rf echoes due to thermal expansion and local changes in the speed of sound. However, there are still many problems to solve before reliable temperature data can be obtained.

The temperature measuring techniques described above have advantages and limitations as to invasive/noninvasive use, resolution, or system size and expense.

This paper discusses a relatively simple multipurpose setup for research that enables the visualization of temperature gradients underneath the surface of a (model) tissue with high spatial and temporal resolution in combination with calibrated temperature measurements.

3 Schlieren Techniques to Visualize Temperature Gradients

The components and strategy of the setup to study laser tissue interaction as shown in Fig. 1 are described below. The basic setup is based on an optical processor using Schlieren techniques. Very small changes in optical density of a medium, induced by temperature gradients or local stresses, are enhanced using spatial filtering.[16,17] The setup is also used for high-speed imaging using microsecond to nanosecond light flashes to study phenomena associated with pulsed lasers. Combining the "thermal imaging" with thermocouple measurements, absolute temperatures can be obtained simultaneously. Descriptions of the technique and components follow.

3.1 Color Schlieren Techniques

An overview of all the components of the setup is shown in Fig. 1. Conceptually, the setup is an optical processor as is schematically shown in Fig. 2. A continuous or pulsed white light source is coupled into a fiber. The light emitted from a ball-shaped tip is focused, providing a point source and divergences subsequently. The focal point of a collimating lens coincides with the focus of the beam. The diameter of the lens is matched with the divergence of the beam so that all light is
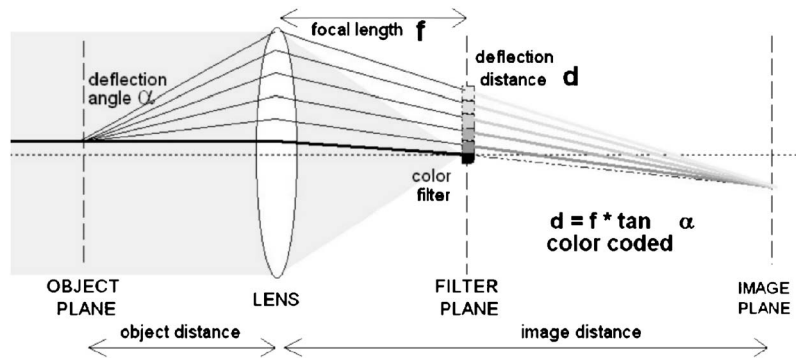
Fig. 2 Scheme of optical processor for spatial filtering using a either a block filter or a color filter.

collimated. A rectangular tank filled with a medium (e.g., water or tissue) is positioned between the collimating and imaging lens, the "object" plane. The walls are perpendicular to the parallel beam to prevent any optical distortion due to refraction. Within this tank, conditions are created to study laser-tissue interaction. The imaging lens will focus the parallel beam in its focal point on the optical axis. However, due to variations in the refraction index or irregularities in the medium in the object plane induced by, for example, temperature gradients or local stresses, rays will be deflected. These rays will cross the focal plane at a particular distance d from the optical axis (Fig. 2). The nondistorted rays will be focused on the optical axis. By inserting a mask or a filter in the focal plane of the imaging lens, it is possible to block out the non-deflected rays, preventing them from reaching the image plane or to earmark rays crossing the plane at certain positions. This process of modifying the object information in the focal plane is known as spatial filtering. By blocking the rays crossing the optical axis, only refracted and diffracted rays will pass the filter plane and contribute to an image restoration at the image plane. The result is an enormous contrast enhancement of the image due to the subtraction of the background light (Fig. 3).

Depending on the deflection angle α and the focal length of the transform lens, a ray will pass the filter plane at a deflection distance d from the optical axis (Fig. 2): $d = f \tan \alpha$. The information on the degree of deflection can be preserved by color coding the rays coming through the filter plane using a color filter (Fig. 4). This filter consists of concentric rings of discrete color bands separated by small black rings. The center of the filter is a black dot blocking the background light. Adjacent to the black dot, with increasing distance from the center, the colors shift gradually from blue to red. Rays passing the filter plane will be color coded depending on the deflection distance d and will be reconstructed to an image at the image plane. The generated color image will show, depending on the position, the degree of deflection in the object plane. From each color, the deflection angle α can be determined; α is related to the change in the refractive index of the medium in the object plane. The color image can be interpreted as a thermal image when the relation between refractive index and temperature gradient is known. The black rings in the filter will result in black lines in the image separating the discrete colors giving an impression of "isotherms" (Fig. 5). The position of the imaging lens, the filter, and the

charge-coupled device (CCD) camera are chosen depending on the magnification desired according to the lens formula. The diameter of the filter determines the dynamical range of temperature gradient that can be visualized. Using an x-y microtranslator, the filter can be optimally aligned on the optical axis. The CCD camera is positioned in the image plane. Additional filters can be used to filter out scattered light from the primary laser wavelength. To obtain microsecond resolution, a video camera with high-speed mode can be used.

3.2 Absolute Temperature Measurements

The color images give a relative impression of temperature distributions as will be discussed in Secs. 3.4 and 7.2. To obtain absolute temperatures, thermocouples are positioned in the field of view. Up to six K-type thermocouples (200 to 600-μm diameter) can be positioned at strategic positions in the tissue being studied to measure the temperature simultaneously during imaging. However, because the thermocouple wires will disturb the image, they are used mostly for calibration of the temperature distribution in a series of experiments (Fig. 6). The readings are acquired with a personal computer (PC) and converted to absolute temperatures.

3.3 Video Processing

A sensitive, high resolution CCD camera is used for imaging. The camera has a wide range of controls as to exposure time, white balance, and frame coding. The video frames are captured and processed in real time by a PC at video frames rate (up to 30 fs).
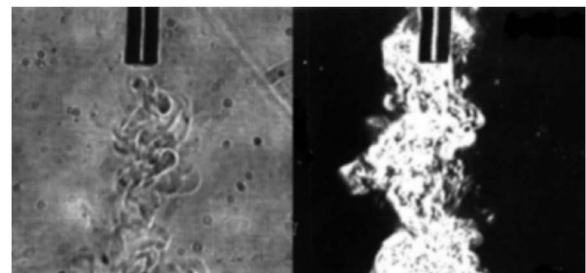

Fig. 3 Example of contrast enhancement using the block filter showing convection of water heated by laser fiber emitting ir light absorbed by water.
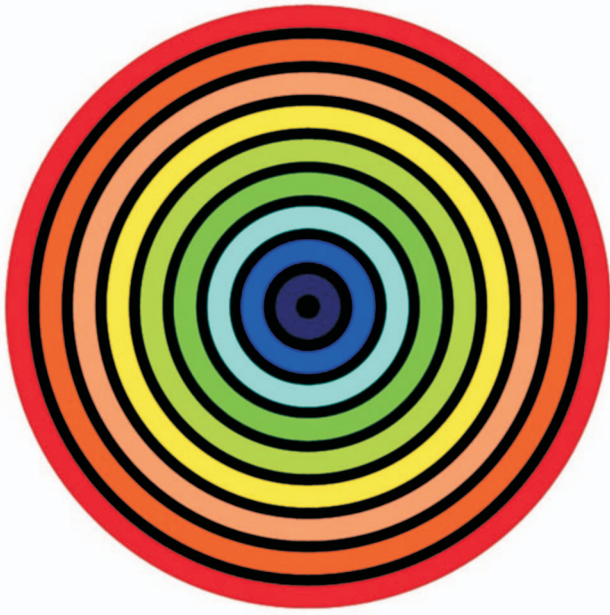
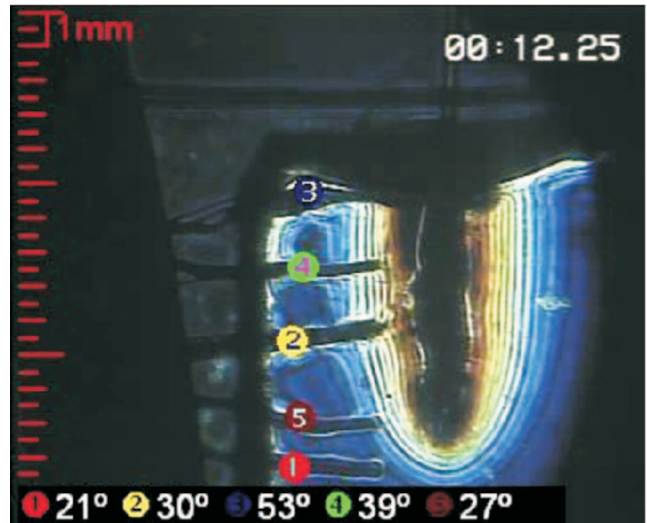**Fig. 4** Example of a ″rainbow″ color filter.

Fig. 6 Example of a thermal image with additional information. The numbered row of dark lines is the shadow of the thermocouples positioned in the transparent tissue at the level of the thermal field. The temperatures of related thermocouples are displayed at the bottom in real time. The image is tagged by a time code and dimensions can be determined.

Additional information is mixed in the video frames:
1. a time code is added giving a unique number to each frame
2. a ruler at the side providing the dimensions in the image
3. markers with number for the position of thermocouples
4. the actual temperature readings from the numbered thermocouples
5. marker indicating that the source is activated

An example of a resulting image is shown in Fig. 6.

3.4 Interpretation of Color Schlieren Images as Thermal Images

The color Schlieren setup as described produces real-time false color images that give the impression of a thermal image. However, assigning absolute temperatures to the colors in the images is complicated. It is important to understand that

Fig. 5 Example of a color coded image showing the thermal zone around an ablation crater during CO_2 laser irradiation. The black lines can be interpreted as isotherms. The left inset shows the normal view.

the images show temperature gradients that refract the parallel light rays. The "calibration" of the color Schlieren images is highly dependent on the symmetry of the temperature field. The theoretical description of the relation between the colors and temperature gradients is discussed in the Appendix.[6]

In summary, if the temperature field is unidirectional (e.g., a hot surface as created by a highly absorbed laser wavelength), the relation between color and temperature can be described by a first order polynomial. If the temperature field has an axial distribution, the temperature is related to a ratio derived from the radius of the temperature gradient field and the position of a point in this field (see Appendix).

Without being able to ascribe temperatures to colors, the images are very useful for relative comparison and study temperature field dynamics.

4 High-Speed Imaging

4.1 High-Speed Schlieren Imaging

In the setup, the Schlieren techniques can be combined with high-speed imaging. First of all, motion in the field of view can be frozen using a high-speed shutter of the video camera itself normally going down to 100 μs. However, a continuous wave white light source will usually not provide sufficient light for a good exposure. High intensity white light pulses from a flash, for example used in photography, can be used if sufficient light can be coupled into the illumination fiber. While using normal video rate exposure of 20 ms, the flash will "freeze" motion with pulse times down to microseconds. For imaging thermal processes, this time range is adequate and can be used to study thermal relaxation times of small structures like blood vessels.

To study the mechanical effects of pulsed lasers, Schlieren techniques can be used for contrast enhancement. To image the microexplosions and shockwaves that are induced by
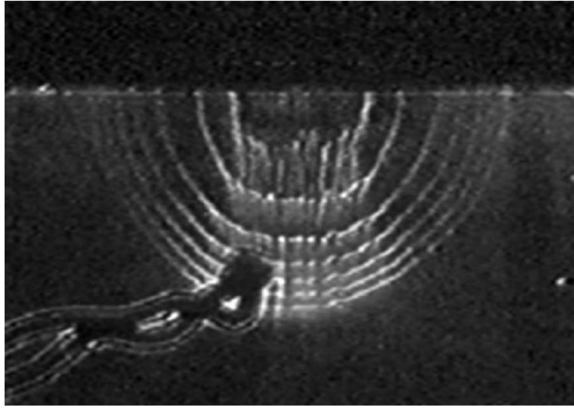
Fig. 7 Multiple exposure of an expanding cavity at a water surface induced by water vapor created by a holmium laser pulse. It shows seven contours, each 100 μs apart.

pulsed lasers in tissue, exposure times down to nanoseconds are needed. The light source suitable to provide light flashes down to the nanosecond or even picosecond region, with efficient light coupling into the illumination fiber, is a pulsed laser in the visible range. Because lasers are monochromatic, the color technique to code the degree of deflection of the parallel rays cannot be used. Instead, quantitative data can be obtained using special design spatial filters or using a multiple wavelength laser, a broadband dye laser, or laser-induced fluorescence light. By controlling the time between the laser pulse interacting with tissue and the light flash for exposure, it is possible to study the dynamics of the interaction in time with a temporal resolution down to nanoseconds. A trigger box drives the light flash for exposure after a preset time delay from the start of the laser pulse interacting with tissue (Fig. 1). By increasing the delay time, a sequence of images of individual laser pulses can be obtained showing the dynamics of the interaction.[18] Using a laser source with a high repetition rate as a flash, it is possible to make stroboscopic images using multiple exposures within one video frame. Figure 7 shows such an image obtained using a copper vapor laser as a light source that emits 10 ns pulses of green-yellow light with a repetition frequency of 10 kHz. During the 1 ms exposure time, 10 flashes, each 100 μs apart, captured the formation of a cavity at a water surface induced by water vapor created by a holmium laser pulse.

4.2 Combination of High-Speed Imaging and Color Schlieren Imaging

Besides imaging in "Schlieren mode," a separate flash, directly illuminating the target, can be used for "normal" high-speed imaging. The same triggering and time delay technique can be applied to capture images during interaction of laser pulses with tissue using a white light flash of several microseconds. Arc lamps in stroboscopes provide 1-μs light flashes with a repetition rate up to several hundred hertz. This enables flash pulse repetition at video rate or multiple exposures within one video frame.

In the setup (Fig. 1), the high-speed and color Schlieren imaging technique can be combined to visualize thermal and mechanical effects during laser-tissue interaction simulta-
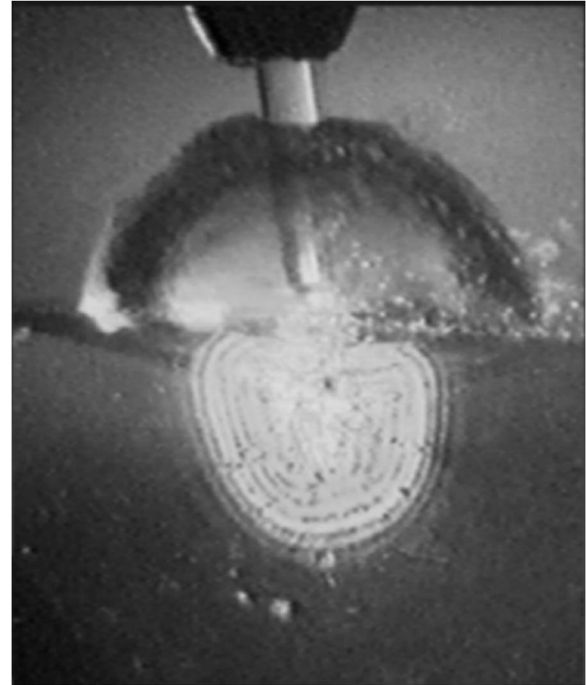

Fig. 8 Combined high-speed and Schlieren image of an explosive vapor bubble during a holmium laser pulse above a tissue area heated by previous pulses.

neously in real time. Figure 8 shows an explosive vapor bubble above the surface of a tissue being heated by previous pulses.

5 Tissue Model to Simulate Laser-Tissue Interaction

For the color Schlieren visualization technique, the light has to pass through a transparent medium in which the laser interacts with the tissue. Therefore the laser-tissue interaction in (living) biological tissues can only be simulated in a transparent model tissue mimicking the properties of biological tissue.
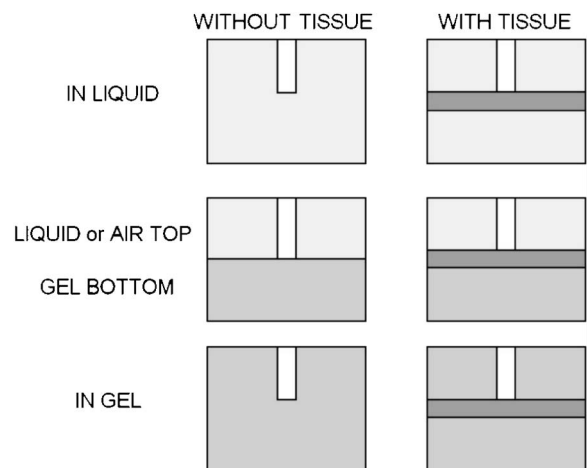

Fig. 9 Conditions to simulate the interaction of a focused or fiber delivered laser beam with the transparent PA tissue model that can be combined with a slab of biological tissue.

Table 1 Overview of studies conducted using the color Schlieren imaging setup.

Specialism	Application	Device	Goal
Basic science	Pulsed lasers		Explosive vapor formation
Basic science	Fiber delivery devices		Thermal characteristics fiber tips
Cardiac surgery	Transmyocardial revascularization	CO_2, holmium, excimer	Comparison of various lasers
Cardiology	Laser revascularization	Nd:YAG, holmium, excimer	Settings for safe application, understanding mechanism action
Dermatology	Skin resurfacing	Pulsed CO_2 with scanner	Settings for optimal application
Dermatology	Hair removal		
Dermatology	Vascular treatments	KTP, pulsed dye	Settings for optimal application
Dermatology	Vascular treatments	KTP, pulsed dye	Effect of surface cooling
ENT surgery	Ablation of defect in throat	Pulsed CO_2	Settings for safe application, effect of focus, and pulse sequences
General surgery	Electrosurgery	Electrosurgery unit	Comparison of applicators, traction speed, and application of argon gas
General surgery	Laser surgery	Nd:YAG, diode, thulium	Comparison of efficiency various fiber tips for cutting
Neurosurgery	Endoscopic third ventriculostomies	Diode thulium	Settings for safe application
Neurosurgery	Tumor resection	CUSA	Understanding mechanism action
Neurosurgery	Nonocclusive bypass surgery in brain	Nd:YAG Excimer	Settings for safe application
Orthopedic surgery	Cartilage remodeling during arthroscopy	Holmium	Settings for safe application, angle of irradiation
Urology	BPH treatment	Nd:YAG, holmium, Side fire fibers	Comparison of various lasers and side firing fibers
Urology	Lithotripsy	Holmium	Settings for safe application in urethra
Urology	BPH treatment	Electrosurgery unit	Comparison of various applicators, traction speed
Vascular surgery	Endovascular laser treatment	Diode, thulium, Nd:YAG	Understanding mechanism action

Polyacrylamide gel (PA) is used as a model tissue. It resembles biological tissue as to the following properties:

1. Thermal properties: Thermal conduction is dominated by the water content of tissue. The PA gel can made with 70 to 90% water content comparable with tissue.
2. Optical properties: Depending on the laser under investigation, the optical properties of the PA gel can be matched with real tissue. For ir lasers >1500 nm, water is the dominant absorber and the PA gel already has the correct optical properties. For the range of visible to near ir, a dye can be added to the gel, which mimics,

depending on concentration, the total effective absorption. For the neodymium:yttrium aluminum garnet (Nd:YAG) (1064 nm) and diode (780 to 820 nm) wavelength, copper sulfate can be used as an absorber. For visible wavelengths, there are many dyes available that are used for the food industry, for example. Scattering particles will undermine the concept of Schlieren techniques. By using the combined effective absorption coefficient (μ_a and μ_s), the scattering properties can partly be compensated. Also in conditions for study,
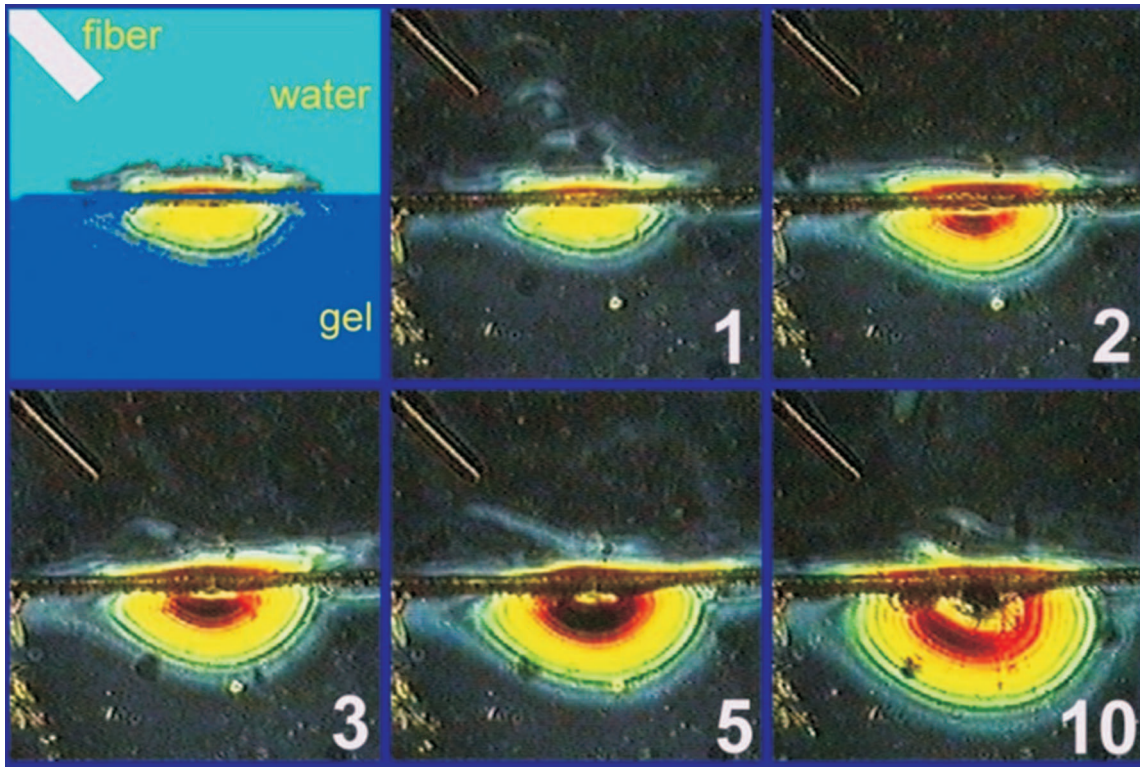
Fig. 10 Orthopedic surgery, cartilage reshaping. Accumulation of heat in tissue after a number of holmium pulses of 0.5 J at 5 Hz.
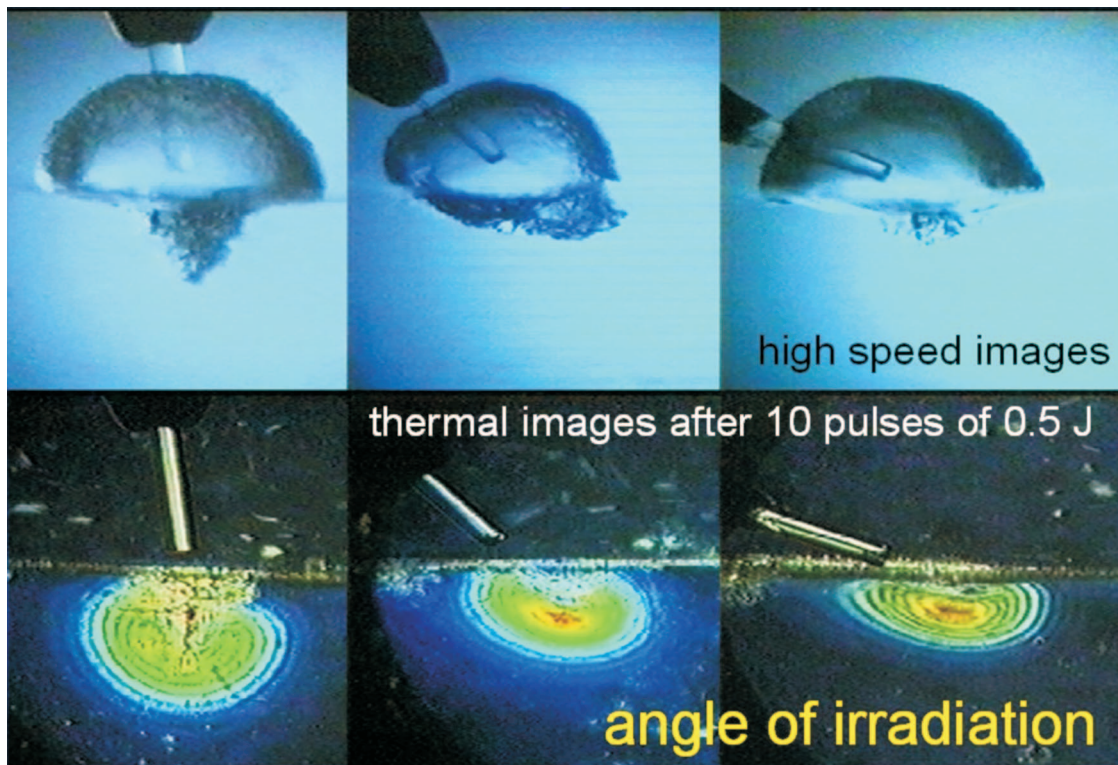

Fig. 11 Orthopedic surgery, cartilage reshaping. Bottom row: Effect of angle or irradiation on the extent of thermal damage in tissue after exposure with 10 holmium pulses of 0.5 J. Top row: High-speed image of explosive vapor bubbles inducing mechanical damage (cracks) to the tissue.
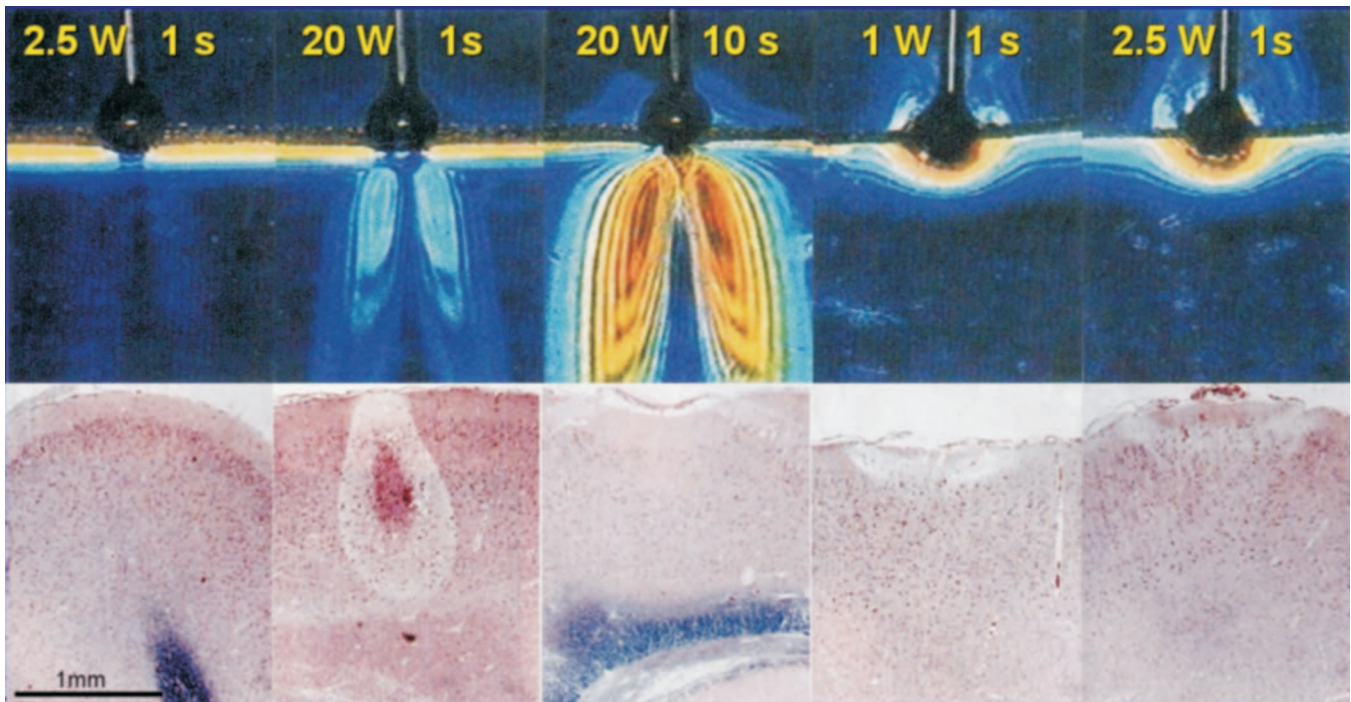
Fig. 12 Neurosurgery, treatment of hydrocephalus. The extent of thermal damage imaged with the color Schlieren technique (top row) and confirmed *in vivo* by Nd:YAG laser exposure of rabbit brain tissue (bottom row) at the settings shown in the images. The first three frames from the left show the effects of an uncoated ball tip. There is no tissue ablation, only undesired deep coagulation. In contrast, the two frames from the right show the effect of a coated ball tip. Already at powers of a few watts, tissue is ablated with minimal thermal damage in the tissue underneath.

scatter effects can be compensated by using a larger beam diameter.

3. Mechanical properties: The PA gel is rather sturdy and elastic and resembles soft biological tissue. It will not melt in contrast to other gels such as gelatin. At higher temperatures, it dehydrates and around $100\,°C$, its wa-

ter content will vaporize leaving a cavity in the gel. At temperatures above $100\,°C$, its polymer structure decomposes and turns brown.

4. Electrical properties: Although not relevant for laser studies, the PA gel can be made of saline instead of water to simulate conduction of electric current, to study the thermal effects of diathermia and rf generators used in medicine.

To overcome some of the limitations of the PA gel during the initial laser-tissue interaction, a thin slab of biological tissue can be put on top or sandwiched between slabs of the PA gel. The heat, generated in the tissue, will be conducted to the gel and will indirectly reflect the temperature distribution in the tissue.

The model tissue is positioned in the object plane of the setup (Fig. 1) to simulate the situation of the *in vivo* laser-tissue interaction as accurately as possible while imaging the temperature field of interest. Figure 9 gives a schematic overview of various conditions to perform the experiments. Either a fiber transporting the laser light is positioned in the field of view above the target tissue or a laser beam is focused on the surface. The target tissue can be liquid, PA gel, or a thin slab of biological tissue. The surrounding can be air, water, or a physiologic media such as blood.
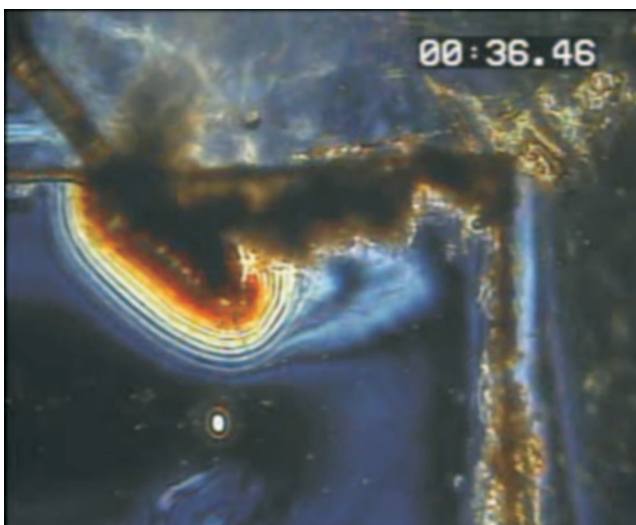

Fig. 13 Urology. This thermal image shows the simulation of BPH treatment, tracking a fiber over the tissue surface using 50 W of cw thulium laser light. The dark area shows the volume of tissue ablated. The extent of thermal effects can be appreciated along this area.

6 Applications of the Imaging Setup

Since the development of the setup, the color Schlieren imaging technique was employed for many studies of tissue interaction with various lasers and other instruments dissipating

Fig. 14 Urology. Similar to Fig. 13, BPH treatment is simulated comparing two power settings of a rf generator coupled to a ball-shaped metal electrode in contact with the tissue. While rolling the ball over the tissue surface at a speed of 2 mm/s a hot "tail" is left behind inside the tissue that is larger for the higher power setting, as can be expected.

Fig. 15 Urology. Simulation of lithotripsy in ureter: a fiber is positioned above a urinary stone in a water-filled lumen with a 3-mm diameter within transparent tissue. After a train of 5 holmium pulses of 0.5 J at 5 Hz, thermal effects can be observed along the channel wall.

energy for treatment. With the introduction of a new medical application, the setup was used to get a better understanding of the mechanism of action. In many cases, it was used to compare different strategies or devices for a particular application. Methods were compared in an objective way, sometimes in cooperation with medical companies. For medical applications in the University Medical Center Utrecht, the setup was used to find the safe and optimal settings for an application. An important advantage of all the studies is the video footage obtained, which is ideal for education and presentations. Instead of explaining the tissue interaction to physicians with complex graphs and formulas, the color video sequences show a realistic representation of the extent of thermal and mechanical effects inside tissue.

In the Table 1, an overview is presented of studies for both research and education in which the color Schlieren setup has been used.

The following paragraphs give representative examples to illustrate the magnitude of this imaging method for various medical applications.

6.1 Orthopedic Surgery: Simulation of Cartilage Reshaping during Arthroscopy

The holmium laser is used for remodeling defects of the cartilage in the knee. The thermal effect of the number of pulses at one position (Fig. 10) and the angle of irradiation (Fig. 11) was studied to obtain the optimum and safe settings for treatment.[19] The imaging showed that irradiating the tissue near perpendicular angles resulted in extensive thermal and mechanical damage. Using the fiber at an angle around 30 deg to the tissue, the explosive vapor bubbles act as a shaver remodeling an irregular surface while the thermal energy molds and seals it.

6.2 Neurosurgery: Treatment of Hydrocephalus

For the treatment of too high fluid pressure in the brain (hydrocephalus), an alternative passage is created to drain the fluid from the brain by fenestration of the floor of the third

ventricle.[20] This procedure was simulated to prove the optimal setting and safety of a specially designed ball-shaped fiber tip with a carbon coating that converts all laser light to thermal energy at the tip.[21] A comparison was made between coated and noncoated fiber tips at various power settings in the brain tissue of a rabbit and imaged using the color Schlieren technique (Fig. 12). This confirmed the efficiency and safety of the coated tips to penetrate through tissue membranes at low power settings.[22] This procedure has been performed successfully in over 300 patients using these "black tip" fibers.

6.3 Urology: Treatment of Benign Prostate Hyperplasia

Benign prostate hyperplasia (BPH) is a common syndrome in elderly males that hinders voiding the bladder. It can be treated effectively by resecting the obstructive part of the prostate within the urethra. Many devices have been developed over the years based on laser and rf energy sources. These devices have been studied extensively using the color Schlieren setup[23–25] and comparing the thermal effects at various parameters such as power, scanning speed, probe design, etc. (Figs. 13 and 14). The images show the ablation area and distribution and dynamics of the thermal energy dissipated in the tissue. Most laser devices proved to be effective for the treatment; however, due to the long learning curve and expensive equipment, most urologists turned back to the "golden standard," transurethral resection of the prostate (TURP), using high power rf generators.
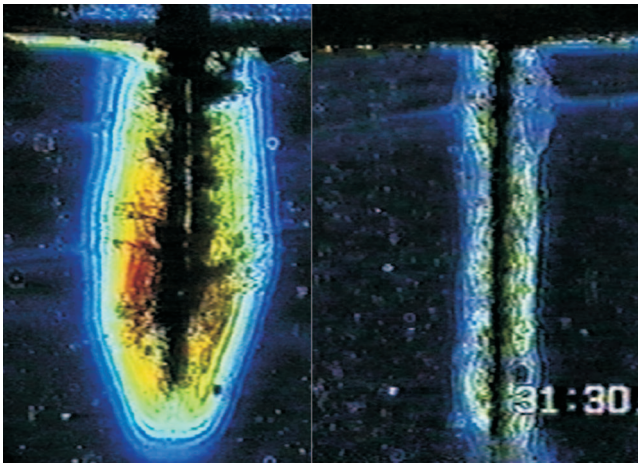
Fig. 16 Cardiac surgery. The thermal effects resulting from the drilling of a long channel in tissue using either a fiber-delivered holmium laser pulse (1 J, 5 Hz, left frame) or a pulse from a focused CO_2 beam (500 mJ, right frame). The channel created by the CO_2 beam is smooth with minimal thermal effects. The wall of the channel created with holmium pulses is irregular and the thermal effects are significant.

6.4 Urology: Safety for Lithotripsy in Ureter

The explosive vapor bubbles created by holmium laser pulses can be effectively applied to break stones in the field of urology. During lithotripsy in the bladder, there is plenty of space for the vapor to expand without damaging the bladder wall. However, when treating a stone in the ureter, the explosive vapor bubble can easily expand beyond the lumen of the ureter overstretching the wall. Using the combined high-speed and thermal imaging setup,[26] it was determined that pulse energy should not exceed 0.5 J and only a train of three pulses at the time should be given to prevent damage to the ureter wall (Fig. 15).
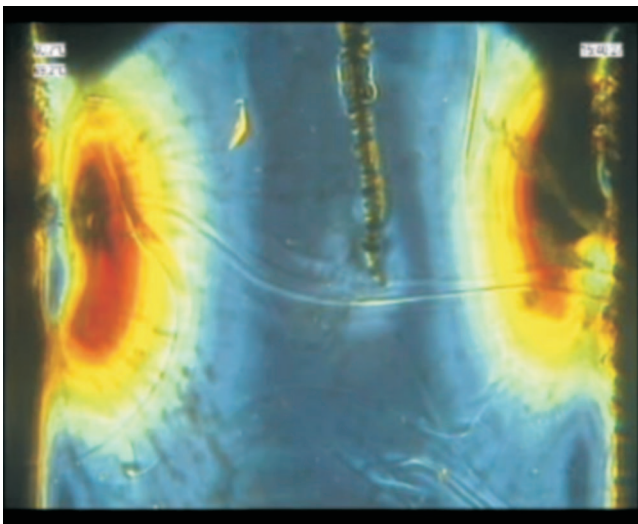

Fig. 20 Quantification. Thermal image of effect of a Nd:YAG beam penetrating deep into the tissue heating a cylindrical volume. Although, the area around the central axis is expected to be hottest, the image shows two hot lobes beside the central axis. This image illustrates that the colors cannot directly be interpreted as temperatures.

Fig. 19 General surgery. Simulation of rf coagulation of liver tumors. The image of the temperature field between the electrodes of two needles on each side of the frame activated in turn with a rf generator.
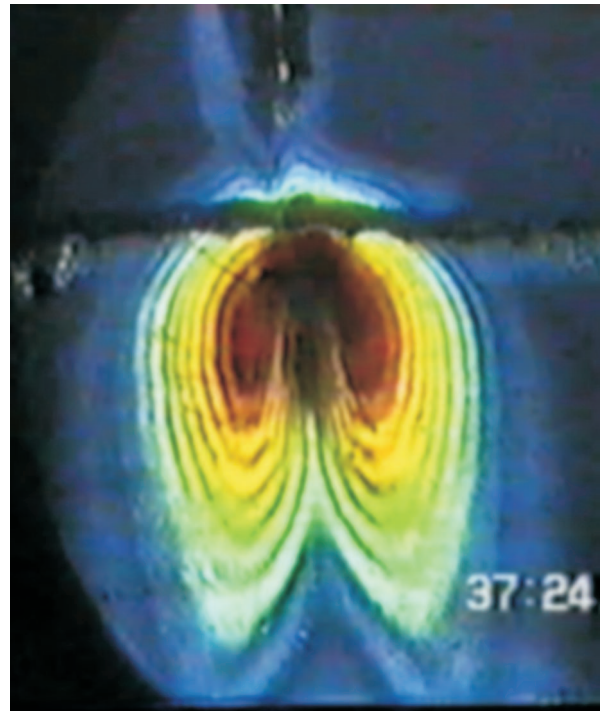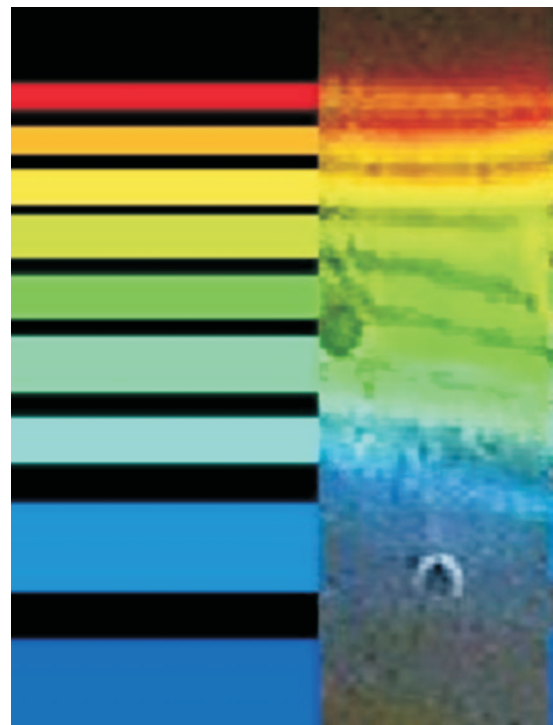

Fig. 21 Quantification. Result from a ray-trace simulation through a unidirectional temperature gradient above a hot surface (left side) compared to "real" color Schlieren image of the same condition (right side). The match between both color bands is significant.
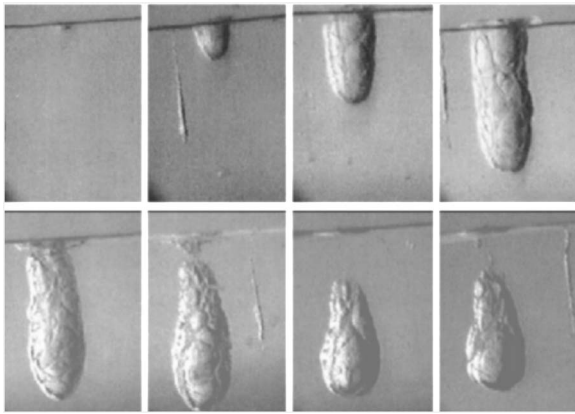
Fig. 17 Cardiac surgery. High-speed sequence of the formation of a channel during a focused CO_2 beam at the surface of a transparent tissue, each frame is 100 μs apart. The explosive vapor creates an opening in the tissue surface enabling the beam to penetrate to deeper layers during a pulse with 500 mJ energy and 1 ms duration.

6.5 Cardiac Surgery: Reviving Hibernating Myocardium by Transmyocardial Revascularization to Relieve Angina Complaints

For several years, reviving hibernating myocardium has been attempted by drilling holes in the tissue to stimulate the formation of new vasculature feeding the myocardium in need of oxygen. Various lasers were used for this goal and the mechanism of action of the lasers was studied using the combined high-speed and thermal imaging setup.[27] It was shown that the mechanical and thermal damage varied significantly between the various lasers and settings (Figs. 16 and 17). However, for the patients the outcome relieved angina complaints dramatically after surgery. After 1 year, complaints returned and the method was consequently abandoned by most cardiac surgeons.

6.6 General Surgery: Working Mechanism of Ultrasound Cavitational Devices

In this study, a hollow titanium needle was used as a resection device for soft tumor tissue, for example, in the liver, was imaged with the high-speed Schlieren setup[28] while the tip was vibrating at ultrasonic velocities in water (Fig. 18). Cavitation bubbles were observed that pulverize soft tissues during their collapse. At the moment of implosion, shock waves were observed that had not been noticed before.

6.7 General Surgery: Coagulation of Large Tumor Areas in the Liver

Secondary tumors affect large volumes over 10 cm in diameter in the liver. Especially when multiple areas are involved, resection is not possible. Instead, the tumors are coagulated by using laser (Nd:YAG, diode) or rf as the thermal energy source. Multiple diffusing fibers or needles with rf electrodes are positioned at strategic positions in the liver to destroy the tumor while preserving the organ structure. The treatment was simulated using the color Schlieren imaging to see the devel-
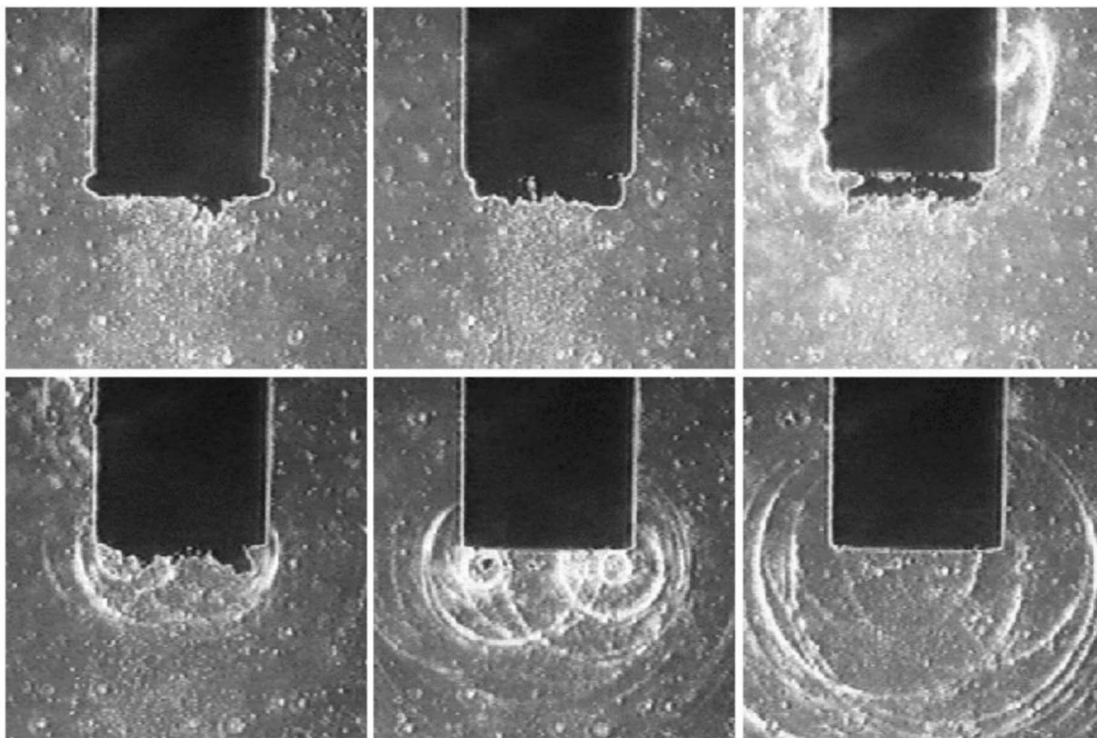

Fig. 18 Neurosurgery, tumor resection. High-speed Schlieren imaging of an instrument creating cavitation bubbles and shock waves [cavitational ultrasonic surgical aspirator (CUSA), Valley Lab, Boulder, CO]. The sequence of frames shows the phases through the duty cycle of 50 μs. Cavitation bubbles are formed underneath the tip of a hollow titanium needle vibrating at ultrasonic speed. At the moment the cavitation bubbles implode, shock waves are visible using Schlieren techniques.
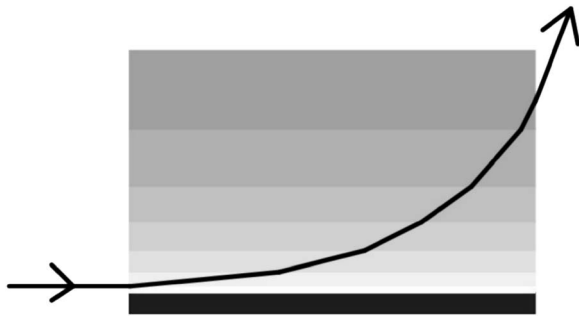
Fig. 22 Deflection of ray in medium with a temperature gradient above a hot surface (unidirectional).

Fig. 23 Graph showing the relation between color (distance to optical axis at filter plane) and temperature in a thermal image of a unidirectional distribution.

opment of the heat distribution in time depending on the power settings and activation sequences of the multiple fibers or electrodes (Fig. 19).

7 Discussion

The setup described in this paper is based on an optical method to enhance contrast of an image using Schlieren techniques. Schlieren techniques are described in all textbooks on fundamental optics. Color filters in Schlieren techniques have been used for various applications.[16] The more sophisticated "rainbow" filter was applied mostly for applications in an air environment.[17] The introduction of the rainbow filter by the authors for applications in physiological media for medical research was original.[3]

7.1 Development of the Setup

The components to build a color Schlieren setup are relatively straightforward and the first images obtained can be impressive. However, it takes more effort to improve the setup. Over the years, the setup was enhanced by using better optics and by matching the focal lengths, magnification, and size of the filter with the degree of refraction of rays in the object plane. The originally photographic rainbow filters were replaced by computer-generated filters, in which black circles were added to separate the colors to enable possibilities for quantification. In the images, these black rings provide an impression of "isotherms."

The video camera was upgraded in time and combined with PC-based video mixing techniques adding information like dimensions, time codes, and temperatures (Fig. 6).

The high-speed imaging option was also added in a later phase. It takes some practice to align the flash light to the optimal position to combine the exposures of the "thermal" image with the "still flash" in one video frame.

7.2 Quantification of Temperature Distributions Visualized

It is important to realize that the images produced are a result of the defection of rays due to a temperature gradient. This gradient is largest during the heating of tissue as long as the source is active. The temperature decrease is usually exponentially away from the source. The largest gradient is near the source, which is reflected by the color coding in the image. As soon as the energy source is turned off, the steepness of the gradient fades away. When the temperature gradient decays, it
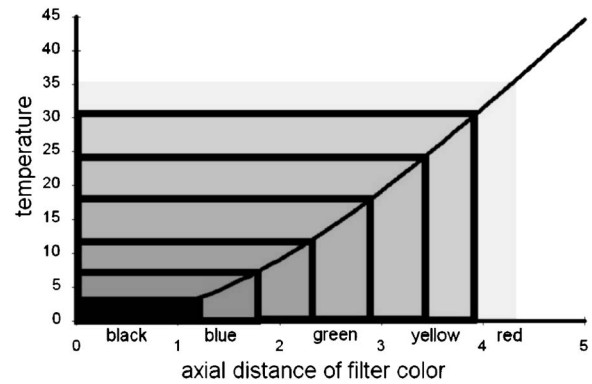
becomes by approximation linear resulting in just one color in the image across the thermal field. This could be interpreted mistakenly as a thermal field of a constant temperature.

In the Appendix, it is shown how the colors can be related to temperatures if the temperature distribution is symmetrical with a presumed geometry that is planar, cylindrical, or spherical. For most conditions, the geometry can be approximated by one of these geometries. The heat source is usually a point, a disk, or half dome. Consequently, the direction of the heat conduction is either unidirectional or radial. For a unidirectional temperature gradient (planar), the relation can be approximated by the first order polynomial. Using a smart distribution of the color rings in the Schlieren filter with the width adjusted for this relationship, it should be possible to produce color images in which the colors represent calibrated temperature ranges.

The axial geometry (spherical or cylindrical) is more difficult to calibrate since it is related to the ratio derived from the radius the temperature gradient field and the position of a point in this field. The result is best illustrated by Fig. 20 where the beam of a Nd:YAG laser penetrates deep into the tissue heating a cylindrical volume of tissue. The thermal image shows two lobes formed from the center. Although, the central axis is hottest, its appearance in color distributions suggests that it is cooler. This example clearly shows one of the pitfalls of this imaging method to interpret the color zones as temperature zones.

To obtain a better understanding of the refraction of light rays due to a temperature gradient in a medium, the path of the rays was simulated by ray tracing.[29] The ray tracing was performed under the symmetrical conditions unidirectional or radial. These conditions were also simulated in the color Schlieren setup so the results could be compared. Figure 21 shows the results from the ray tracing next to an image of a unidirectional temperature gradient above a hot surface. The match between both color bands is significant. Similar results can be obtained for the radial symmetry. However, these ideal temperate distributions can easily be disturbed by convection and turbulence. From that moment, it becomes too complex to relate colors to temperatures. Due to the high contrast and detail, the qualitative images obtained with this visualization technique are still useful for studying thermal transport and fluid dynamics.
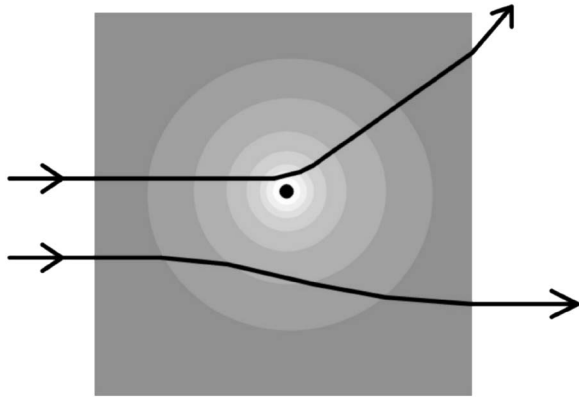
Fig. 24 Deflection of rays in a medium with a radial temperature distribution.

7.3 Thermocouple Measurements

To overcome the limitation of relating colors to real temperatures, thermocouples can be positioned at representative positions in the field of view, such as the axis of symmetry of the expected temperature field. However, the thermocouples are invasive and disturb the field of view. Pushing the wires into the model tissue creates small cracks that are clearly visible in the image since this imaging technique is very sensitive for small disturbances. The temperatures from the thermocouples are superposed in real time onto the captured images. Showing calibrated temperatures of some positions in the color images is a useful addition that makes the need for calibration of the colors less necessary.

7.4 Qualitative Comparison using Color Schlieren Imaging

Although the use of color Schlieren imaging is limited for quantitative temperature imaging, it is useful for conducting comparative studies. For example, thermal distributions and relaxation times can be visualized comparing various systems

or system settings without the need for absolute temperatures. Many studies have been conducted this way as is shown in Table 1.

7.5 Tissue Model

It is essential that the tissue to be transparent for this imaging method. The only biological tissue that would meet these conditions would be the vitreous humor of the eyeball. However, due to its jelly substance, it is difficult to work with and also hard to obtain in large quantities. Any transparent model will lack the scattering properties of tissue. Even the smallest quantity of scattering material in the model tissue would blur the image and make it useless. The high sensitivity of the technique for optical "irregularities" is in this sense a disadvantage. To overcome this limitation, a slab of real biological tissue can be used with a thickness limited to the effective penetration depth for the wavelength studied, sandwiched between slabs of the transparent model tissue (Fig. 9, right column). The initial scattering and absorption takes place in this tissue layer and the heat generated will be conducted to the gel and become visible by the Schlieren color coding. If the absorption is high and dominates scattering, one can use an absorber dissolved in the model tissue as long as it is transparent for the visual range of wavelengths. Such absorbers are available both the uv and near ir (Nd:YAG).

7.6 Educational Tool

Despite several limitations of the color Schlieren technique to study laser-tissue interaction as discussed above, the most important advantage is its value for education. The movie clips obtained of the dynamics during laser-tissue interaction are self-explaining even for novices in this area of research. Although, the laser-tissue interactions cannot be simulated in detail, the essence can be mimicked to show a good representation of reality. The imaging has proven to be very effective for education and training of students, scientists, and physicians. Even professionals in this area of research have shown their appreciation for this imaging technique as it shows the basic essentials of laser-tissue interactions.
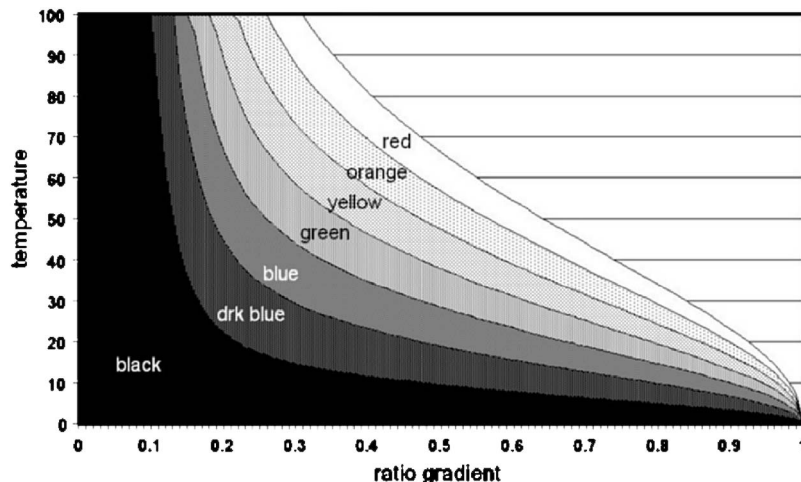

Fig. 25 Relation between color and temperature in color image with a radial temperature distribution.

7.7 *Areas for Application*

As shown in the overview of applications (Table 1), this imaging technique is not limited to studying laser interactions with tissue. Any energy source generating heat or mechanical effects in tissue can be studied. As shown, imaging was obtained of rf devices and ultrasound devices generating cavitation bubbles.

8 Conclusions

An optical setup combining color Schlieren techniques and high-speed imaging techniques can successfully be applied to visualize thermal and mechanical phenomenon in model tissues with high spatial and temporal resolution. This method is a useful tool for studying the thermal effects of cw and pulsed lasers during interaction with biological tissues. For symmetric temperature distributions and with additional thermocouple measurements, it is possible to interpret color Schlieren images as thermal images within an acceptable accuracy. The real-time color images provide a good understanding of thermodynamics and thermal relaxation during laser-tissue interaction with cw and pulsed lasers. This setup has proven to be a great education tool for researchers, surgeons, nurses, and students.

APPENDIX

1 Calibration of Setup

To interpret the color image as a temperature image, the relation between color and temperature should be calibrated. There is a direct relation between the deflection distance d and the color depending on the size of the filter. The relation of the deflection distance and the temperature: $d=f(t)$ depends on (1) the angle of deflection α, (2) the focal length of imaging lens, (3) the object distance, (4) the image distance, and (5) the symmetry of the refractive index distribution.

The symmetry of the refractive index distribution is of major importance. This calibration can only be performed by assuming a particular symmetry. One can approximate the distributions by a unidirectional or an axially symmetrical distribution.

2 Unidirectional Refractive Index Distribution

This situation occurs in the case of a temperature gradient above a heated surface (Fig. 22) and can be considered a one-dimensional situation. An example of the calibration curve for a unidirectional temperature distribution is given in Fig. 23.

3 Axially Symmetric Refractive Index Distribution

This situation occurs in the case of a temperature gradient around a "hot spot" in a cylindrical or spherical geometry and can be considered a two-dimensional situation (Fig. 24).

An example of the calibration curve for an axially symmetric temperature distribution is given in Fig. 25. This graph is difficult to interpret. The temperature at a particular position in an image has to be determined from the color and the ratio of the temperature gradient. This ratio is the distance from the axis of symmetry (usually the highest temperature) divided by the distance over which the temperature gradient extends [from the axis of symmetry to ambient temperature (black)].

4 Calibration Measurements

Unidirectional and cylindrical temperature gradients (Figs. 22 and 24) were created by heat dissipation from an electrical current through carbon plates and rods (0.5 to 3.0 mm diameter) in an aqueous medium while being imaged with the color Schlieren method. The absolute temperatures were determined by scanning a 0.1-mm diameter thermocouple through the gradient and the results were compared to theoretical expected values. There was a good fit between data and theory for the unidirectional gradient (Fig. 23). For the cylindrical gradient, the fit depended on the orientation (vertical or horizontal) of the carbon rods due to convection. For a larger diameter of the rod, the cylindrical temperature gradient resembles the unidirectional gradient.

References

1. A. L. McKenzie, "Physics of thermal processes in laser-tissue interaction," *Phys. Med. Biol.* **35**, 1175–1209 (1990).
2. J. H. Torres, T. A. Springer, A. J. Welch, and J. A. Pearce, "Limitations of a thermal camera in measuring surface temperature of laser-irradiated tissues," *Lasers Surg. Med.* **10**, 510–523 (1990).
3. R. M. Verdaasdonk, "Imaging laser induced thermal fields and effects," in Laser-Tissue Interaction VI, S. L. Jacques, Ed., *Proc. SPIE* **2391**, 165–175 (1995).
4. P. Carnochan, R. J. Dickinson, and M. C. Joiner, "The practical use of thermocouples for temperature measurement in clinical hyperthermia," *Int. J. Hyperthermia* **2**, 1–19 (1986).
5. K. Ramanathan and B. Danielsson, "Principles and applications of thermal biosensors," *Biosens. Bioelectron.* **16**, 417–423 (2001).
6. F. Lammers and T. Scheper, "Thermal biosensors in biotechnology," *Adv. Biochem. Eng./Biotechnol.* **64**, 35–67 (1999).
7. R. M. Verdaasdonk, F. C. Holstege, E. D. Jansen, and C. Borst, "Temperature along the surface of modified fiber tips for Nd:YAG laser angioplasty," *Lasers Surg. Med.* **11**, 213–222 (1991).
8. L. J. Jiang, E. Y. Ng, A. C. Yeo, S. Wu, F. Pan, W. Y. Yau, J. H. Chen, and Y. Yang, "A perspective on medical infrared imaging," *J. Med. Eng. Technol.* **29**, 257–267 (2005).
9. B. F. Jones, "A reappraisal of the use of infrared thermal image analysis in medicine," *IEEE Trans. Med. Imaging* **17**, 1019–1027 (1998).
10. B. Denis de Senneville, B. Quesson, and C. T. Moonen, "Magnetic resonance temperature imaging," *Int. J. Hyperthermia* **21**, 515–531 (2005).
11. B. Quesson, J. A. de Zwart, and C. T. Moonen, "Magnetic resonance temperature imaging for guidance of thermotherapy," *J. Magn. Reson Imaging* **12**, 525–533 (2000).
12. Y. Leroy, B. Bocquet, and A. Mamouni, "Non-invasive microwave radiometry thermometry," *Physiol. Meas* **19**, 127–148 (1998).

13. G. T. Clement and K. Hynynen, "Ultrasound phase-contrast transmission imaging of localized thermal variation and the identification of fat/tissue boundaries," *Phys. Med. Biol.* **50**, 1585–1600 (2005).

14. M. Pernot, M. Tanter, J. Bercoff, K. R. Waters, and M. Fink, "Temperature estimation using ultrasonic spatial compound imaging," *IEEE Trans. Ultrason. Ferroelectr. Freq. Control* **51**, 606–615 (2004).

15. R. M. Arthur, J. W. Trobaugh, W. L. Straube, and E. G. Moros, "Temperature dependence of ultrasonic backscattered energy in motion-compensated images," *IEEE Trans. Ultrason. Ferroelectr. Freq. Control* **52**, 1644–1652 (2005).

16. G. S. Settles, "Color Schlieren Optics—A review of techniques and applications," in *Flow Visualization*, Vol. **2**, W. Merzkirch, Ed., pp. 749–759, Hemisphere, New York (1982).

17. W. L. Howes, "Rainbow Schlieren and its applications," *Appl. Opt.* **23**, 2449–2460 (1984).

18. T. G. van Leeuwen, M. J. van der Veen, R. M. Verdaasdonk, and C. Borst, "Non-contact tissue ablation by holmium:YSGG laser pulses in blood," *Lasers Surg. Med.* **11**, 26–34 (1991).

19. M. C. M. Grimbergen, R. M. Verdaasdonk, and C. F. P. van Swol, "Correlation of thermal and mechanical effects of the holmium laser for various clinical applications," *Proc. SPIE* **3254**, 69–79 (1998).

20. W. P. Vandertop, R. M. Verdaasdonk, and C. F. P. van Swol, "Laser-assisted neuroendoscopy using Nd:YAG and diode contact laser with pretreated fiber tips," *J. Neurosurg.* **88**, 82–92 (1998).

21. R. M. Verdaasdonk, W. P. Vandertop, W. Ansink, and C. F. P. van Swol, "Laser-assisted neuroendoscopy using Nd:YAG and Diode contact laser with 'black' fiber tips," *Proc. SPIE* **2970**, 591–598 (1997).

22. P. W. A. Willems, W. P. Vandertop, R. M. Verdaasdonk, C. F. P. van Swol, and G. H. Jansen, "Contact laser-assisted neuroendoscopy can be performed safely by using pretreated 'black' fiber tips: experimental data," *Lasers Surg. Med.* **28**, 324–329 (2001).

23. C. F. P. van Swol, R. J. van Vliet, R. M. Verdaasdonk, and T. A. Boon, "Electrovaporization as a treatment modality for transurethral resection of the prostate: influence of generator type," *Urology* **53**, 317–321 (1999).

24. C. F. P. van Swol, R. M. Verdaasdonk, and T. A. Boon, "Prostate on the menu: an overview of cooking techniques and clinical outcome," *Proc. SPIE* **2975**, 234–239 (1997).

25. C. F. P. van Swol, R. M. Verdaasdonk, R. J. van Vliet, D. G. Molenaar, and T. A. Boon, "Side-firing devices for laser prostatectomy," *World J. Urol.* **13**, 88–93 (1995).

26. C. F. P. van Swol, R. M. Verdaasdonk, B. Zeijlemaker, and T. A. Boon, "Optimalization of the dosimetry and safety using the holmium laser for urology," *Proc. SPIE* **3245**, 110–116 (1998).

27. R. M. Verdaasdonk, "Transmyocardial revascularization: the magic of drilling holes in the heart," in *Matching the Energy Source to the Clinical Need*, T. P. Ryan, Ed., Critical Reviews, Vol. CR75, pp. 99–135, SPIE, Bellingham (2000).

28. R. M. Verdaasdonk, C. F. P. van Swol, M. C. M. Grimbergen, and G. Priem, "High-speed and thermal imaging of the mechanism of action of the Cavitational Ultrasonic Surgical Aspirator (CUSA)," *Proc. SPIE* **3249**, 72–84 (1998).

29. R. M. Verdaasdonk, R. Lodder, C. F. P. van Swol, and M. C. M. Grimbergen, "Thermal imaging of laser-tissue interaction using color Schlieren techniques quantified by ray-tracing simulation," *Proc. SPIE* **3601**, 156–165 (1999).